

Two-component cyclotron resonance in quantum Hall systems

Kenichi Asano and Tsuneya Ando

Institute for Solid State Physics, University of Tokyo, 7-22-1 Roppongi, Minato-ku, Tokyo 106, Japan

(Received 9 February 1998)

Effects of electron-electron interactions on spin-split and mass-split cyclotron resonance (CR) in a quantum Hall regime are studied by means of numerical diagonalization in finite-size systems. In the case of spin-split CR, the spectra at low temperatures show a simple mode-repulsion behavior at low filling factors, while they show more complicated behaviors at high filling factors including motional narrowing when the electron density for up-spin and that for down-spin are comparable. The spectra at high temperatures can be understood in terms of increase in the effective filling factor. The results qualitatively explain experiments in GaAs/Al_xGa_{1-x}As heterostructures. In the case of mass-split CR, the spectra show only a mode-repulsion behavior independent of temperatures and filling factors. [S0163-1829(98)06627-2]

I. INTRODUCTION

Cyclotron resonance is known to provide important information on electronic properties in two-dimensional systems (2DES's) in high magnetic fields. In a homogeneous system where each electron has a same cyclotron frequency, CR spectra are not influenced by electron-electron interactions (Kohn's theorem).¹ In fact, the external electric field couples only with the center-of-mass motion unaffected by internal forces and equivalent to a single harmonic oscillator with the cyclotron frequency ω_0 . In an inhomogeneous or multicomponent system, however, Kohn's theorem is no longer valid and electron-electron interactions directly modify CR spectra. The purpose of this paper is to study effects of electron-electron interactions on two-component CR in 2DES's by means of numerical diagonalization of the Hamiltonian for finite-size systems.

In 1970's the Si (001) inversion layer was studied. In this system, there are two different sets of subbands with different cyclotron masses. The first set is twofold degenerate subbands $\epsilon_0, \epsilon_1, \dots$ formed at two valleys in the [001] direction and the second set is fourfold degenerate subbands $\epsilon'_0, \epsilon'_1, \dots$ formed at the other four valleys. At high temperatures where both ϵ_0 and ϵ'_0 subbands are occupied by electrons, only a single peak was observed in CR.² A uniaxial stress was applied in the [100] (or [010]) direction to lower the ϵ'_0 subband, but only a single peak was observed.³ Two CR peaks were observed in later more elaborate experiments under higher stresses and at higher electron densities.^{4,5}

Motivated by these interesting experiments, CR in Si inversion layers was studied theoretically. Landau's Fermi-liquid theory gave the result that CR spectra can be regarded as two coupled modes that repel each other in the presence of electron-electron interactions leading to a transfer of intensities between the modes (a mode repulsion).⁶⁻⁸ The effective coupling constant between two CR modes is determined by a dimensionless Fermi-liquid parameter. A mechanism based on electron-electron collisions was also proposed,⁹ which is present only at nonzero temperature and make each kind of electrons relax to a state with a common velocity. This friction effect makes two CR peaks merge together with the increase of collisions (a motional narrowing).

Since the 1980's, CR in GaAs/Al_xGa_{1-x}As heterostructures has been intensively studied. The CR spectrum in bulk GaAs systems exhibits two kinds of splittings caused by non-parabolicity effect. In fact, the cyclotron frequency for the transition from the N th to $(N+1)$ th Landau level for a σ -spin ($\sigma = \uparrow, \downarrow$) electron have σ dependence because the g factor or the Zeeman splitting has slight energy dependence.¹⁰ It also depends on the Landau-level index N due to the energy dependence of the effective mass.¹¹ The former is called spin or Δg splitting and the latter is called mass or Δm splitting. However, no clear evidence of either spin or mass splitting was found in GaAs/Al_xGa_{1-x}As heterostructures with electron density $n \sim 10^{11} \text{ cm}^{-2}$ in a magnetic field $B \sim 10 \text{ T}$.¹²⁻¹⁶

Only recently, spin splittings were observed in samples in the extreme quantum limit¹⁷⁻²⁰ or in a very high magnetic field.²¹ In these experiments,¹⁷⁻²⁰ CR shows an intriguing dependence on the filling factor ν and temperature. At $\nu < 1/10$, two peaks are observed and their positions are independent of temperature, while only a single peak is observed at $\nu > 1/6$. A crossover between these two types of behavior occurs at $\nu \sim 1/9$, where two peaks merge into a single peak with decreasing temperature.

Effects of electron-electron interactions on spin-split CR were studied theoretically for $\nu \ll 1/10$ where electrons are believed to form a hexagonal Wigner solid.²² It was later supplemented by a study based on a coherent potential approximation.²³ These results seem to explain the experimental results qualitatively if being extrapolated up to $\nu \sim 1/10$.

Electron-electron interactions play an important role also in mass-split CR.^{15,16,24} A theoretical study in a generalized single mode approximation²⁴ (GSMA) predicted some anomaly that an effective coupling constant between two CR modes corresponding to transitions from $N=0$ to 1 and from $N=1$ to 2 changes its sign when the first excited Landau level is nearly half-filled.

In this paper, we study these spin-split and mass-split cyclotron resonances by numerically diagonalizing the Hamiltonian in 2DES's consisting of a finite number of electrons. It is organized as follows: In Sec. II, the models and the method of calculations are discussed and in Sec. III GSMA

is reviewed briefly. The obtained results are presented in Sec. IV and discussed in Sec. V. A summary and conclusion are given in Sec. VI. A preliminary account of a part this work at a very early stage has been presented.²⁵

II. MODEL AND METHOD

A. Electrons on torus

Let us consider a 2DES with a rectangular form $S=a \times b$ where a and b are the linear dimension in the x and y direction, respectively. The system contains N_e electrons with charge $-e$ ($e>0$). We shall use periodic boundary conditions in both x and y directions. The area of the system is not arbitrary but given by

$$S=2\pi l^2 N_\phi, \quad (2.1)$$

where l is the magnetic length defined by $l=\sqrt{\hbar/eB}$ and N_ϕ is an integer that gives the number of magnetic flux quanta passing through the system. The total filling factor is defined by

$$\nu=\frac{N_e}{N_\phi}. \quad (2.2)$$

In the following, we shall confine ourselves to the case of the presence of a small nonparabolicity in the conduction band. The nonparabolicity is assumed to give rise to only a slight shift of the energy of Landau levels. Strictly speaking, a nonparabolicity leads to a mixing of different Landau levels and spins, and therefore various transitions other than conventional CR corresponding to those between adjacent Landau levels with the same spin can be induced such as an electric-dipole induced spin resonance. Usually this nonparabolicity effect on electron wave functions is much smaller than that on energy levels except in the case of a strong nonparabolicity.

In a Landau gauge $\mathbf{A}(\mathbf{r})=(0,Bx)$, the wave function of a single electron is given by $\phi_{Nj}(\mathbf{r})\chi_\sigma$, where $\phi_{Nj}(\mathbf{r})$ is the spatial wave function and χ_σ is the spinor of σ -spin state. The spatial wave function $\phi_{Nj}(\mathbf{r})$ is written explicitly as

$$\begin{aligned} \phi_{Nj}(\mathbf{r}) &= \left(\frac{1}{2^N N! \sqrt{\pi b l}} \right)^{1/2} \\ &\times \sum_{m=-\infty}^{\infty} H_N \left(\frac{X_j + ma - x}{l} \right) \\ &\times \exp \left[-i \frac{(X_j + ma)y}{l^2} - \frac{(X_j + ma - x)^2}{2l^2} \right], \end{aligned} \quad (2.3)$$

where H_N is the Hermite polynomial and X_j is the x coordinate of the guiding center, which takes discrete N_ϕ values

$$X_j = \frac{2\pi l^2}{b} j, \quad (j=0,1,\dots,N_\phi-1). \quad (2.4)$$

The Hamiltonian is written as

$$\begin{aligned} \mathcal{H} &= \sum_{\xi} \epsilon_{N\sigma} c_{\xi}^{\dagger} c_{\xi} + \frac{1}{2S} \\ &\times \sum_{\mathbf{q} \neq 0} \sum_{\xi_1 \xi_2 \xi_3 \xi_4} \frac{e^2}{2\epsilon|\mathbf{q}|} \delta_{\sigma_1 \sigma_4} \delta_{\sigma_2 \sigma_3} (N_1 j_1 | e^{-i\mathbf{q}\cdot\mathbf{r}} | N_4 j_4) \\ &\times (N_2 j_2 | e^{i\mathbf{q}\cdot\mathbf{r}} | N_3 j_3) c_{\xi_1}^{\dagger} c_{\xi_2}^{\dagger} c_{\xi_3} c_{\xi_4}, \end{aligned} \quad (2.5)$$

where \mathbf{q} is the reciprocal wave vector given by $\mathbf{q}=(2\pi n_x/a, 2\pi n_y/b)$ with n_x and n_y being integers and c_{ξ}^{\dagger} and c_{ξ} are the creation and destruction operator, respectively, for the state with index $\xi=(N,j,\sigma)$. The nonparabolicity appears only in $\epsilon_{N\sigma}$, which is slightly different from $(N+\frac{1}{2})\hbar\omega_0+(\frac{1}{2})g\mu_B B\sigma$ depending on N and σ , where ω_0 is the cyclotron frequency given by $\omega_0=eB/m$ with an effective mass m , μ_B is the Bohr magneton, and g is the g factor. The matrix element is given by

$$\begin{aligned} (Nj | e^{i\mathbf{q}\cdot\mathbf{r}} | N'j') &= \int_0^a dx \int_0^b dy \phi_{Nj}^*(\mathbf{r}) e^{i\mathbf{q}\cdot\mathbf{r}} \phi_{N'j'}(\mathbf{r}) \\ &= e^{-|\mathbf{q}|^2 l^2 / 4} A_{NN'}(\mathbf{q}) B_{jj'}(\mathbf{q}), \end{aligned} \quad (2.6)$$

with

$$A_{NN'}(\mathbf{q}) = \begin{cases} \sqrt{\frac{N'!}{N!}} \left[\frac{(iq_x + q_y)l}{\sqrt{2}} \right]^{N-N'} L_{N'}^{N-N'} \left(\frac{|\mathbf{q}|^2 l^2}{2} \right) & (N \geq N'), \\ \sqrt{\frac{N!}{N'!}} \left[\frac{(iq_x - q_y)l}{\sqrt{2}} \right]^{N'-N} L_N^{N'-N} \left(\frac{|\mathbf{q}|^2 l^2}{2} \right) & (N < N') \end{cases}, \quad (2.7)$$

and

$$\begin{aligned} B_{jj'}(\mathbf{q}) &= \int_0^a dx \int_0^b dy \phi_{Nj}^*(\mathbf{r}) e^{i\mathbf{q}\cdot\mathbf{R}} \phi_{Nj'}(\mathbf{r}) \\ &= \delta'_{n_y, j' - j} \exp \left[\frac{i\pi}{N_\phi} n_x (j + j') \right], \end{aligned} \quad (2.8)$$

where L_n^m is an associated Laguerre polynomial, $\mathbf{R}=[il^2(\partial/\partial y), y - il^2(\partial/\partial x)]$ is the guiding center coordinate, and $\delta'_{j,j'}$ is defined by

$$\delta'_{j,j'} = \begin{cases} 1 & (j \equiv j' \pmod{N_\phi}), \\ 0 & (\text{otherwise}). \end{cases} \quad (2.9)$$

The total current operator is written as

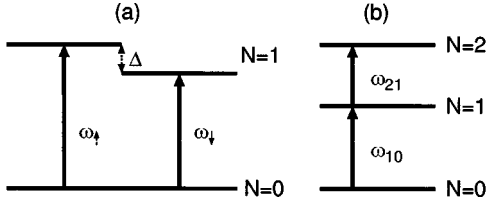


FIG. 1. A schematic illustration of the (a) spin- and (b) mass-split cyclotron resonance. Up-spin electrons have a larger cyclotron frequency than down-spin electrons in (a) and the energy between the lowest and the first excited Landau level is larger than that between the first and the second excited Landau level in (b).

$$J^{\pm} = J_x \pm iJ_y = \pm i\sqrt{2}el\omega_0 \sum_{N\sigma} A_{N\sigma}^{\pm}, \quad (2.10)$$

with

$$A_{N\sigma}^{+} = \sqrt{N+1} \sum_{j=0}^{N_{\phi}-1} c_{N+1,j,\sigma}^{\dagger} c_{N,j,\sigma}, \quad (2.11)$$

$$A_{N\sigma}^{-} = \sqrt{N+1} \sum_{j=0}^{N_{\phi}-1} c_{N,j,\sigma}^{\dagger} c_{N+1,j,\sigma}.$$

The strength of the Coulomb interaction is characterized by the effective Coulomb energy E_C defined by

$$E_C = \frac{e^2}{4\pi\epsilon l}, \quad (2.12)$$

where ϵ is the static dielectric constant. In the following we shall consider the strong-field limit, $E_C \ll \hbar\omega_0$, in which mixing between different Landau levels due to the Coulomb interaction can be neglected. We assume also that $k_B T \ll \hbar\omega_0$, where T is the temperature and k_B is the Boltzmann constant.

The many-body states written as

$$c_{\xi_1}^{\dagger} c_{\xi_2}^{\dagger} \cdots c_{\xi_N}^{\dagger} |\text{vac}\rangle \quad (2.13)$$

form a complete set of normalized orthogonal basis, where $|\text{vac}\rangle$ is the vacuum state. Diagonalization of the Hamiltonian matrix represented by these basis gives us all eigenenergies and eigenstates in the finite-size system. It is known that this numerical diagonalization method is very useful to study low-energy excitations of fractional quantum Hall effect.^{26–28}

Although the periodic boundary conditions break the continuous translational symmetry, a discrete translational symmetry still survives in the Hamiltonian (2.5). Using this symmetry, the Hamiltonian can be block diagonalized and each block is indexed by Haldane's wave vector.²⁹ This wave vector is conserved in the optical transitions because the current operator commutes with the magnetic translation operators.

B. Spin-split cyclotron resonance

The model of spin-split CR is shown in Fig. 1(a). In this case, there are up-spin (\uparrow) and down-spin (\downarrow) electrons in the lowest Landau level ($N=0$). They have a cyclotron frequency slightly different from each other, i.e.,

$$\begin{aligned} \omega_{\uparrow} &= \omega_0 + \frac{\Delta}{2}, \\ \omega_{\downarrow} &= \omega_0 - \frac{\Delta}{2}, \end{aligned} \quad (2.14)$$

where $\Delta \ll \omega_0$. The dimensionless coupling parameter is defined by

$$\alpha = \frac{E_C}{\hbar\Delta}. \quad (2.15)$$

In the initial states, the lowest Landau level is partially filled by N_{\uparrow} up-spin electrons and N_{\downarrow} down-spin electrons. In the final states, a single up- or down-spin electron is excited into the first excited Landau level. The filling factor of electrons with spin σ is defined by

$$\nu_{\sigma} = \frac{N_{\sigma}}{N_{\phi}}. \quad (2.16)$$

The CR spectra for circularly polarized light are determined by the real part of a dynamical conductivity,

$$\sigma(\omega) = \sigma_{xx}(\omega) + i\sigma_{xy}(\omega).$$

Using the Kubo formula, the normalized CR spectrum is calculated in the leading order of Δ/ω_0 , $E_C/\hbar\omega_0$, and $k_B T/\hbar\omega_0$ as

$$\begin{aligned} P(\tilde{\omega}) &\equiv \frac{\text{Re}[\sigma(\omega)]}{\sigma_0} \\ &= \sum_{i,f} \frac{1}{N_e Z} \exp\left(-\frac{E_i}{k_B T}\right) |\langle f | (A_{0\uparrow}^{\dagger} + A_{0\downarrow}^{\dagger}) | i \rangle|^2 \\ &\quad \times \delta\left(\tilde{\omega} - \frac{E_f - E_i - \hbar\omega_0}{\hbar\Delta}\right), \end{aligned} \quad (2.17)$$

where $\tilde{\omega} = (\omega - \omega_0)/\Delta$, Z is the partition function, $|i\rangle$ and E_i are the initial states and their energies, respectively, $|f\rangle$ and E_f are the final states and their energies, respectively, and σ_0 is defined by

$$\sigma_0 = \frac{\nu e^2}{\hbar} \cdot \frac{\omega_0}{2\Delta}. \quad (2.18)$$

We can see that $P(\tilde{\omega})$ satisfies the following sum rules:

$$I_{\text{tot}} = \int_{-\infty}^{+\infty} P(\tilde{\omega}) d\tilde{\omega} = 1, \quad (2.19)$$

and

$$\tilde{\omega}_m = \int_{-\infty}^{+\infty} \tilde{\omega} P(\tilde{\omega}) d\tilde{\omega} = \frac{p}{2}, \quad (2.20)$$

where p is defined by

$$p = \frac{\nu_{\uparrow} - \nu_{\downarrow}}{\nu}, \quad (2.21)$$

which is proportional to the z component of the total spin.

The relative occupation of different spins is determined by the condition of the minimum free energy and varies as a function of the temperature, the g factor or the Zeeman energy, and the strength of the Coulomb interaction.^{30,31} In the following, however, we shall treat ν_\uparrow and ν_\downarrow as parameters independent of others as we are interested in the global behavior of CR spectra as a function of these parameters. Finding an equilibrium spin configuration can be a separate problem.

C. Mass-split cyclotron resonance

The model of mass-split CR is shown in Fig. 1(b). In this case, we neglect electron spins and consider a spinless system. The cyclotron frequencies corresponding to transitions from $N=0$ to $N=1$ and from $N=1$ to $N=2$ have different values ω_{10} and ω_{21} , respectively;

$$\begin{aligned}\omega_{10} &= \omega_0 + \frac{\Delta}{2}, \\ \omega_{21} &= \omega_0 - \frac{\Delta}{2},\end{aligned}\quad (2.22)$$

where $\Delta \ll \hbar\omega_0$. In the initial states, the lowest Landau level is completely filled and the first excited Landau level is partially filled by N_p electrons. In the final states, a single electron in the lowest or the first-excited Landau level is excited into the first or the second excited Landau level, respectively. The filling factor of the first excited Landau level of electrons and holes are defined by

$$\nu_p = \frac{N_p}{N_\phi} \quad (2.23)$$

and

$$\nu_h = \frac{N_h}{N_\phi} = 1 - \nu_p, \quad (2.24)$$

respectively, where $N_h = N_\phi - N_p$ is the number of holes in the first excited Landau level.

In the leading order of Δ/ω_0 , $E_C/\hbar\omega_0$, and $k_B T/\hbar\omega_0$, the normalized dynamical conductivity is written as

$$\begin{aligned}P(\bar{\omega}) &\equiv \frac{\text{Re}[\sigma(\omega)]}{\sigma_0} \\ &= \sum_{i,f} \frac{1}{N_e Z} \exp\left(-\frac{E_i}{k_B T}\right) |\langle f | (A_0^+ + A_1^+) | i \rangle|^2 \\ &\quad \times \delta\left(\bar{\omega} - \frac{E_f - E_i - \hbar\omega_0}{\hbar\Delta}\right).\end{aligned}\quad (2.25)$$

We can also see that $P(\bar{\omega})$ satisfies sum rules (2.19) and (2.20), if p is redefined as

$$p = \frac{\nu_h - 2\nu_p}{\nu}. \quad (2.26)$$

III. SINGLE MODE APPROXIMATION

A. Spin-split cyclotron resonance

In a generalized single-mode approximation (GSMA), two-component CR at absolute zero temperature is regarded as two coupled harmonic oscillators. The absorption spectra are calculated from a 2×2 effective Hamiltonian, which is determined by an effective coupling constant calculated using the guiding-center structure factor in the ground state. The spectra consist of two δ functions and show a mode-repulsion behavior.

In the case of spin-split CR, it is assumed that the f -sum rule (2.19) is exhausted by only two final states which are written as linear combinations of two collectively excited states

$$\begin{aligned}|\uparrow\rangle &= \frac{1}{\sqrt{N_\uparrow}} A_{0\uparrow}^+ |\phi_0\rangle, \\ |\downarrow\rangle &= \frac{1}{\sqrt{N_\downarrow}} A_{0\downarrow}^+ |\phi_0\rangle,\end{aligned}\quad (3.1)$$

where $|\phi_0\rangle$ is the ground state with energy E_0 and $A_{0\sigma}^+$ is defined by Eq. (2.11). The 2×2 effective Hamiltonian is given by

$$\begin{aligned}\mathcal{H}_{\text{eff}} &= \begin{pmatrix} \langle \uparrow | \mathcal{H} | \uparrow \rangle - E_0 & \langle \uparrow | \mathcal{H} | \downarrow \rangle \\ \langle \downarrow | \mathcal{H} | \uparrow \rangle & \langle \downarrow | \mathcal{H} | \downarrow \rangle - E_0 \end{pmatrix} \\ &= \begin{pmatrix} \hbar\omega_\uparrow + \frac{\nu_\downarrow}{\nu} \alpha_{\text{eff}} \hbar\Delta & -\frac{\sqrt{\nu_\uparrow \nu_\downarrow}}{\nu} \alpha_{\text{eff}} \hbar\Delta \\ -\frac{\sqrt{\nu_\uparrow \nu_\downarrow}}{\nu} \alpha_{\text{eff}} \hbar\Delta & \hbar\omega_\downarrow + \frac{\nu_\uparrow}{\nu} \alpha_{\text{eff}} \hbar\Delta \end{pmatrix}.\end{aligned}\quad (3.2)$$

The effective coupling constant α_{eff} is defined as

$$\frac{\alpha_{\text{eff}}}{\alpha} = -\frac{\nu}{\nu_\uparrow \nu_\downarrow} \frac{1}{N_\phi} \sum_{\mathbf{q}} S_{\uparrow\downarrow}(\mathbf{q}) \frac{|\mathbf{q}|l}{2} \exp\left(-\frac{|\mathbf{q}|^2 l^2}{2}\right), \quad (3.3)$$

with the guiding-center structure factor between up- and down-spin electrons in the lowest Landau level given by

$$S_{\uparrow\downarrow}(\mathbf{q}) = \frac{1}{N_\phi} \langle \phi_0 | \rho_\uparrow^{00}(\mathbf{q}) \rho_\downarrow^{00}(-\mathbf{q}) | \phi_0 \rangle, \quad (3.4)$$

where $\rho_\sigma^{00}(\mathbf{q})$ is the Fourier component of the guiding-center density operator of electrons with spin σ in the lowest Landau level given by

$$\rho_\sigma^{00}(\mathbf{q}) = \sum_{jj'} B_{jj'}(\mathbf{q}) c_{0,j,\sigma}^\dagger c_{0,j',\sigma}. \quad (3.5)$$

The coupling parameter α_{eff} has been shown to be positive definite.³²

Diagonalizing this effective Hamiltonian, we obtain the CR spectrum as

$$P(\bar{\omega}) = I_+ \delta(\bar{\omega} - \bar{\omega}_+) + I_- \delta(\bar{\omega} - \bar{\omega}_-), \quad (3.6)$$

where the peak positions $\bar{\omega}_\pm$ and the intensities I_\pm are defined by

$$\tilde{\omega}_{\pm} = \frac{1}{2}(\alpha_{\text{eff}} \pm \sqrt{1 - 2p\alpha_{\text{eff}} + \alpha_{\text{eff}}^2}), \quad (3.7)$$

and

$$I_{\pm} = \pm \frac{\tilde{\omega}_m - \tilde{\omega}_{\mp}}{\tilde{\omega}_+ - \tilde{\omega}_-}. \quad (3.8)$$

In infinite systems ($a, b \rightarrow \infty$), the structure factor has the particle-hole symmetry

$$S_{\uparrow\downarrow}(\mathbf{q}, \nu_{\uparrow}, \nu_{\downarrow}) = S_{\uparrow\downarrow}(\mathbf{q}, 1 - \nu_{\uparrow}, 1 - \nu_{\downarrow}). \quad (3.9)$$

In finite systems, this symmetry is broken because the guiding-center coordinate X is discretized and the electron density distribution is still inhomogeneous when the Landau level is completely filled. However, this finite-size effect is negligible in sufficiently large systems such as $N_{\phi} \geq 4$. The symmetrized effective coupling constant is defined by

$$\alpha_{\text{sym}} = \frac{\nu_{\uparrow}\nu_{\downarrow}\alpha_{\text{eff}}}{\nu} = \frac{\nu(1-p^2)\alpha_{\text{eff}}}{4}, \quad (3.10)$$

which has the particle hole symmetry in the sufficiently large systems:

$$\alpha_{\text{sym}}(\nu_{\uparrow}, \nu_{\downarrow}) = \alpha_{\text{sym}}(1 - \nu_{\uparrow}, 1 - \nu_{\downarrow}). \quad (3.11)$$

The effective coupling constant has also a symmetry with respect to the exchange of up and down spins, i.e.,

$$\alpha_{\text{eff}}(\nu_{\uparrow}, \nu_{\downarrow}) = \alpha_{\text{eff}}(\nu_{\downarrow}, \nu_{\uparrow}), \quad (3.12)$$

$$\alpha_{\text{sym}}(\nu_{\uparrow}, \nu_{\downarrow}) = \alpha_{\text{sym}}(\nu_{\downarrow}, \nu_{\uparrow}),$$

because $S_{\uparrow\downarrow}(\mathbf{q})$ is invariant under this operation.

When the up-spin Landau level is completely occupied, i.e., $\nu_{\uparrow} = 1$, the structure factor $S_{\uparrow\downarrow}(\mathbf{q})$ vanishes. More generally, we have $S_{\uparrow\downarrow} \propto (1 - \nu_{\uparrow})$ for $\nu_{\uparrow} \sim 1$. This leads to the conclusion that the CR spectrum is not influenced by electron-electron interactions in GSMA for $\nu_{\uparrow} = 1$ and $\nu_{\downarrow} < 1$ at all. The same is true in the case that $\nu_{\downarrow} = 1$ and $\nu_{\uparrow} < 1$, although this case is somewhat unrealistic.

At $\nu = 1, \frac{1}{3}, \frac{1}{5}, \dots$, the ground state is believed to be fully spin polarized and α is independent of p , which is proportional to the z component of total electron spin, if the spin Zeeman energy is completely neglected. At $\nu = 1$, in particular, the value of α_{eff} can be calculated analytically as

$$\frac{\alpha_{\text{eff}}}{\alpha} = \sqrt{\frac{\pi}{8}} = 0.6266 \dots, \quad (3.13)$$

because the spatial wave function of the ground state can be written as a single determinant at this filling factor as shown in Appendix A. On the other hand, in the extremely low filling factors such as $\nu \ll 1/10$, it is expected that the system forms a hexagonal Wigner solid and α_{eff} can also be calculated analytically as^{22,33}

$$\frac{\alpha_{\text{eff}}}{\alpha} = \frac{1}{2} \left(\frac{\sqrt{3}\nu}{4\pi} \right)^{3/2} \sum_{\mathbf{l} \neq 0} |\mathbf{l}|^{-3} = 0.2823 \dots \times \nu^{3/2}, \quad (3.14)$$

where $\mathbf{l} = (n + m/2, \sqrt{3}m/2)$ with n and m being an integer as shown in Appendix B. In other cases, the structure factor is calculated for the ground state obtained by exact diagonal-

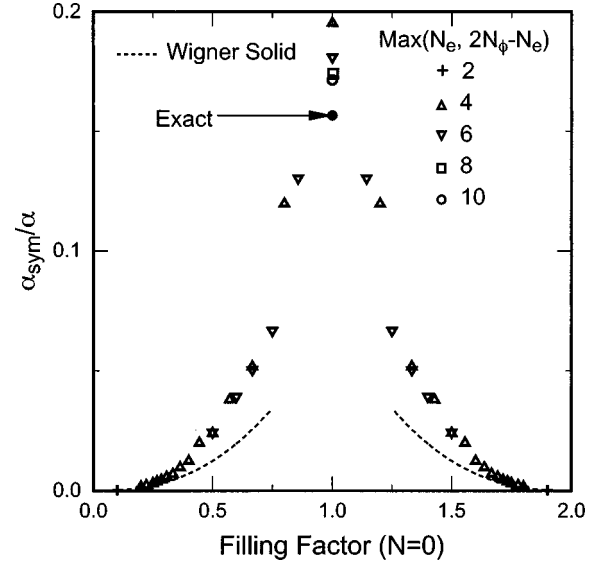


FIG. 2. Calculated ν dependence of effective coupling constant α_{sym} . They are calculated in 2–10 electron (or hole) systems under the condition $p=0$ ($N_{\uparrow} = N_{\downarrow}$). The analytically calculated values at $\nu=1$ and $\nu \ll 1$ are also shown.

ization for finite-size systems. The calculated $\alpha_{\text{sym}}/\alpha$ in the case $\nu_{\uparrow} = \nu_{\downarrow}$ obtained for $2 \leq N_e \leq 10$ are shown in Fig. 2 together with the analytic results given above. The symmetrized coupling constant $\alpha_{\text{sym}}/\alpha$ increases rapidly with ν and reaches a maximum at $\nu=1$.

B. Mass-split cyclotron resonance

In the case of mass-split CR,²⁴ two collectively excited states corresponding to Eq. (3.1) are written as

$$|10\rangle = \frac{1}{\sqrt{N_h}} A_0^+ |\phi_0\rangle, \quad (3.15)$$

$$|21\rangle = \frac{1}{\sqrt{2N_p}} A_1^+ |\phi_0\rangle,$$

where $|\phi_0\rangle$ is the ground state of the system with energy E_0 and A_N^+ is defined by Eq. (2.11). The 2×2 effective Hamiltonian is given by

$$\mathcal{H}_{\text{eff}} = \begin{pmatrix} \langle 10 | \mathcal{H} | 10 \rangle - E_0 & \langle 10 | \mathcal{H} | 21 \rangle \\ \langle 21 | \mathcal{H} | 10 \rangle & \langle 21 | \mathcal{H} | 21 \rangle - E_0 \end{pmatrix} = \begin{pmatrix} \hbar\omega_{10} + \frac{2\nu_p}{\nu} \alpha_{\text{eff}} \hbar \Delta & -\frac{\sqrt{2\nu_p\nu_h}}{\nu} \alpha_{\text{eff}} \hbar \Delta \\ -\frac{\sqrt{2\nu_p\nu_h}}{\nu} \alpha_{\text{eff}} \hbar \Delta & \hbar\omega_{21} + \frac{\nu_h}{\nu} \alpha_{\text{eff}} \hbar \Delta \end{pmatrix}. \quad (3.16)$$

The effective coupling constant α_{eff} is defined by

$$\frac{\alpha_{\text{eff}}}{\alpha} = -\frac{\nu}{\nu_p \nu_h} \frac{1}{N_\phi} \sum_{\mathbf{q}} S_{ph}(\mathbf{q}) \frac{|\mathbf{q}|l}{2} \times \left[1 - \frac{(|\mathbf{q}|l)^2}{4} \right] \exp\left(-\frac{|\mathbf{q}|^2 l^2}{2}\right), \quad (3.17)$$

with $S_{ph}(\mathbf{q})$ being the the guiding-center structure factor between electrons and holes in the first excited Landau level given by

$$S_{ph}(\mathbf{q}) = \frac{1}{N_\phi} \langle \phi_0 | \rho_p^{11}(\mathbf{q}) \rho_h^{11}(-\mathbf{q}) | \phi_0 \rangle, \quad (3.18)$$

where $\rho_p^{11}(\mathbf{q})$ and $\rho_h^{11}(\mathbf{q})$ are the Fourier components of the guiding-center density operator of electrons and holes, respectively, in the first excited Landau level, given by

$$\rho_p^{11}(\mathbf{q}) = \sum_{jj'} B_{jj'}(\mathbf{q}) c_{1,j}^\dagger c_{1,j'}, \quad (3.19)$$

and

$$\rho_h^{11}(\mathbf{q}) = \sum_{jj'} B_{jj'}(\mathbf{q}) c_{1,j'} c_{1,j}^\dagger. \quad (3.20)$$

Diagonalizing this effective Hamiltonian, we obtain the CR spectrum in the same form as Eqs. (3.6)–(3.8). Similarly to the case of spin-split CR, the structure factor is calculated using the ground state $|\phi_0\rangle$ obtained by an exact diagonalization for finite-size systems.

In both finite and infinite size systems, $S_{ph}(\mathbf{q})$ have a particle-hole symmetry. Thus, we can introduce a symmetrized coupling constant as

$$\alpha_{\text{sym}} = \frac{\alpha_{\text{eff}}}{\nu}, \quad (3.21)$$

which has the particle-hole symmetry

$$\alpha_{\text{sym}}(\nu_p) = \alpha_{\text{sym}}(1 - \nu_p). \quad (3.22)$$

In the Hartree-Fock approximation, α_{sym} is independent of ν_p and calculated as $\alpha_{\text{sym}}^{\text{HF}}/\alpha = \sqrt{\pi}/128 = 0.1566 \dots$.²⁴

Figure 3 gives calculated $\alpha_{\text{sym}}/\alpha$ for $2 \leq N_p \leq 10$. It stays positive for all values of ν_p and depends on ν_p only weakly. In fact, it is close to $\alpha_{\text{sym}}^{\text{HF}}/\alpha$ obtained in the Hartree-Fock approximation. In Ref. 24, the effective coupling parameter α_{sym} has been calculated with the use of a Jastrow-type trial wave function and a hypernetted chain method. According to their results, it changes its sign from positive to negative and therefore CR spectra change their behavior from a ‘‘positive’’ mode repulsion to a ‘‘negative’’ mode repulsion around $\nu_p \sim 1/2$. Such an anomaly does not appear in the present results.

IV. NUMERICAL RESULTS

A. Spin-split cyclotron resonance ($T=0$)

Numerical calculations are performed under the condition $2 \leq N_0 \leq 8$, where $N_0 = \text{Min}(N_e, 2N_\phi - N_e)$ means the number of electrons for $\nu \leq 1$ and of holes for $\nu > 1$. We choose $a/b = N_0/4$ according to previous calculations.²⁶ The obtained CR spectra show little dependence on N_0 and a/b if

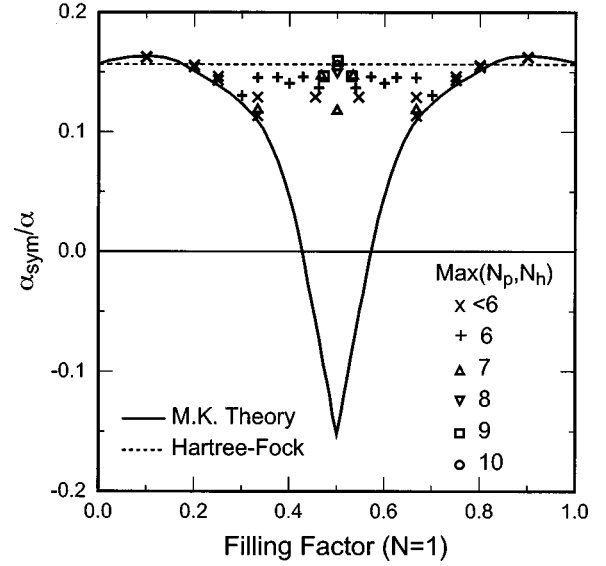


FIG. 3. The ν_p dependence of effective coupling constant α_{sym} . They are calculated in 2–10 electron (or hole) systems. The broken line shows the value calculated in the Hartree-Fock approximation. The result of Ref. 24 is shown by the solid line.

$N_0 \geq 4$ and $a/b \sim 1$. The calculated results are shown by the histograms with width $\Delta/100$ and spectra broadened by a Lorentzian with half-width $\Delta/5$. At zero temperature, the spectra calculated in GSMA and those obtained by a convolution with a Lorentzian with half-width $\Delta/5$ are also shown. Figure 4 gives ν_\uparrow and ν_\downarrow values where the calculations are performed. The parameters are summarized in Table I.

Figure 5 shows the dependence of CR spectra on the coupling constant $\alpha = E_C/\hbar\Delta$ at the low filling factor $\nu = 1/4$ and at zero temperature. The CR spectra consist essentially of two δ functions and show a ‘‘positive’’ mode-repulsion behavior, i.e., when the electron-electron interactions are in-

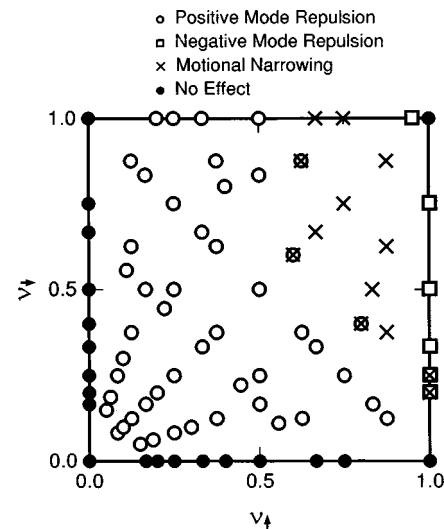


FIG. 4. The value of $(\nu_\uparrow, \nu_\downarrow)$ where calculations are performed. White circles, crosses, and squares mean that the dependence of the $T=0$ spectra on $\alpha = (e^2/4\pi\epsilon l)/\hbar\Delta$ show a positive mode repulsion, a motional narrowing, and a negative mode repulsion, respectively. Black circles show the points where the spectra are independent of electron-electron interactions.

TABLE I. The values of parameters used in the calculations of spin-split CR for the results explicitly shown in the figures.

ν	ν_{\uparrow}	ν_{\downarrow}	p	N_{\uparrow}	N_{\downarrow}	N_0	N_{ϕ}
	$\frac{3}{16}$	$\frac{1}{16}$	$\frac{1}{2}$	3	1	4	16
$\frac{1}{4}$	$\frac{1}{8}$	$\frac{1}{8}$	0	2	2	4	16
	$\frac{1}{16}$	$\frac{3}{16}$	$-\frac{1}{2}$	1	3	4	16
	$\frac{3}{4}$	$\frac{1}{4}$	$\frac{1}{2}$	6	2	8	8
1	$\frac{1}{2}$	$\frac{1}{2}$	0	4	4	8	8
	$\frac{1}{4}$	$\frac{3}{4}$	$-\frac{1}{2}$	2	6	8	8
	1	$\frac{1}{5}$	$\frac{2}{3}$	5	1	4	5
$\frac{6}{5}$	$\frac{3}{5}$	$\frac{3}{5}$	0	3	3	4	5
	$\frac{1}{5}$	1	$-\frac{2}{3}$	1	5	4	5
	1	$\frac{1}{2}$	$\frac{1}{3}$	10	5	5	10
$\frac{3}{2}$	$\frac{3}{4}$	$\frac{3}{4}$	0	6	6	4	8
	$\frac{1}{2}$	1	$-\frac{1}{3}$	4	8	4	8
	1	$\frac{3}{4}$	$\frac{1}{7}$	8	6	2	8
$\frac{7}{4}$	$\frac{7}{8}$	$\frac{7}{8}$	0	7	7	2	8
	$\frac{3}{4}$	1	$-\frac{1}{7}$	6	8	2	8

creased, the higher frequency peak is pushed away toward the higher-frequency side and its intensity is transferred to the lower-frequency peak. They are reproduced well by GSMA.

Figure 6 shows the α dependence of CR spectra at an intermediate filling factor $\nu=1$ and at zero temperature. In this case, the spectra consist of many δ functions, in particular, for $1 \leq \alpha \leq 2$. However, the spectra broadened by a Lorentzian still have essentially two-peak structures and may be categorized as a positive mode-repulsion behavior. The deviation from GSMA results becomes significant in the region $\nu_{\uparrow} \gg \nu_{\downarrow}$.

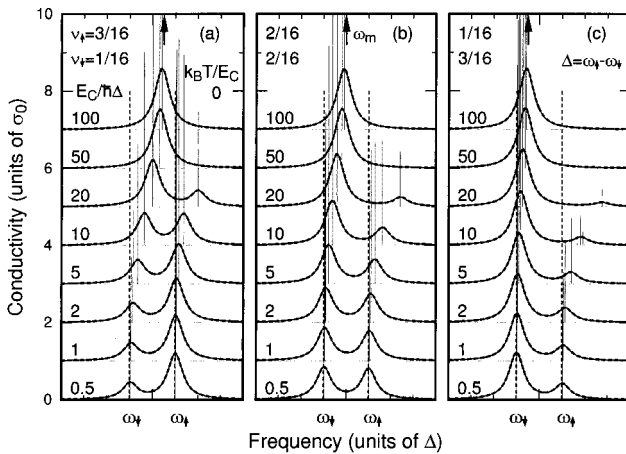


FIG. 5. The dependence of spin-split CR on α at $T=0$ for $\nu = \frac{1}{4}$ in four electron systems. The thin dotted lines represent the histogram with width $\Delta/100$, the solid lines broadened by a Lorentzian with half-width $\Delta/5$, and the broken lines GSMA results broadened by the same Lorentzian. (a) $(\nu_{\uparrow}, \nu_{\downarrow}) = (\frac{3}{16}, \frac{1}{16})$, (b) $(\frac{1}{8}, \frac{1}{8})$, and (c) $(\frac{1}{16}, \frac{3}{16})$.

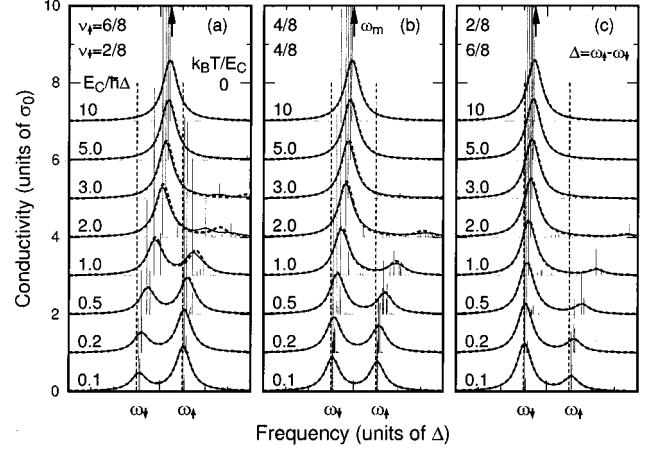


FIG. 6. The α dependence of spin-split CR spectra at $T=0$ for $\nu=1$ in eight electron systems. (a) $(\nu_{\uparrow}, \nu_{\downarrow}) = (\frac{3}{4}, \frac{1}{4})$, (b) $(\frac{1}{2}, \frac{1}{2})$, and (c) $(\frac{1}{4}, \frac{3}{4})$.

Figure 7 shows the results for $\nu = \frac{6}{5}$, Fig. 8 for $\nu = \frac{3}{2}$, and Fig. 9 for $\nu = \frac{7}{4}$. Although the spectra consist of a large number of CR peaks, their behavior can effectively be regarded as two coupled CR modes in the presence of a large broadening. However, the deviation of the spectrum from the GSMA result becomes more and more significant with increasing ν .

When the up-spin Landau level is completely filled ($\nu_{\uparrow} = 1$), i.e., in Figs. 7(a), 8(a), and 9(a), the CR spectra can be categorized as a “negative” mode repulsion, in which the peak in the low-frequency side is shifted toward the high-frequency side and its intensity is transferred to the peak in the high-frequency side. This result is quite in contrast to the GSMA result that shows no effect of electron-electron interactions because of the vanishing coupling constant α_{eff} as mentioned in Sec. III A.

When the number of up- and down-spin electrons is the same ($\nu_{\uparrow} = \nu_{\downarrow}$), the CR spectra change their features from a positive mode repulsion to a “motional narrowing” behavior with increasing ν . In the latter case, two peaks merge together into a single peak as in Fig. 8(b) or a new central peak appears and becomes dominant as in Fig. 9(b), with the increase of the strength of electron-electron interactions. When the down-spin Landau level is completely filled and the up-spin level is partially occupied ($\nu_{\downarrow} = 1$ and $\nu_{\uparrow} < 1$), the positive mode repulsion behavior for $\nu = \frac{6}{5}$ shown in Fig. 7(c) gradually turns into a motional narrowing behavior for $\nu = \frac{7}{4}$ shown in Fig. 9(c) with the increase of ν .

In summary, the CR spectra change their features sensitively as a function of the filling factor of up- and down-spin electrons and exhibit complicated behaviors at high filling factors. Figure 4 summarizes the characteristic CR features in the $(\nu_{\uparrow}, \nu_{\downarrow})$ plane. The positive mode repulsion appears in the region $\nu < 1$ or in $\nu_{\uparrow} \lesssim 1/2$. The negative mode-repulsion appears in the region $\nu_{\uparrow} \sim 1$ and the motional narrowing appears in the region given by the conditions $\nu > 1$ and $1/2 < \nu_{\uparrow} < 1$.

B. Spin-split cyclotron resonance ($T \neq 0$)

The obtained spectra consist of a tremendously large number of δ functions especially at high temperatures. How-

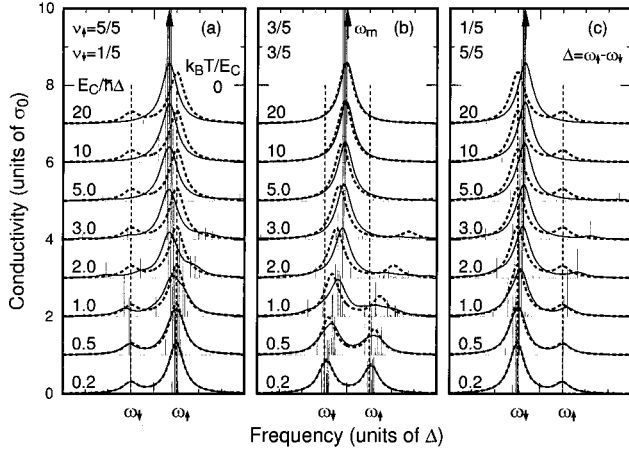


FIG. 7. The α dependence of spin-split CR spectra at $T=0$ for $\nu = \frac{6}{5}$ in four hole systems. (a) $(\nu_{\uparrow}, \nu_{\downarrow}) = (1, \frac{1}{5})$, (b) $(\frac{3}{5}, \frac{3}{5})$, and (c) $(\frac{1}{5}, 1)$.

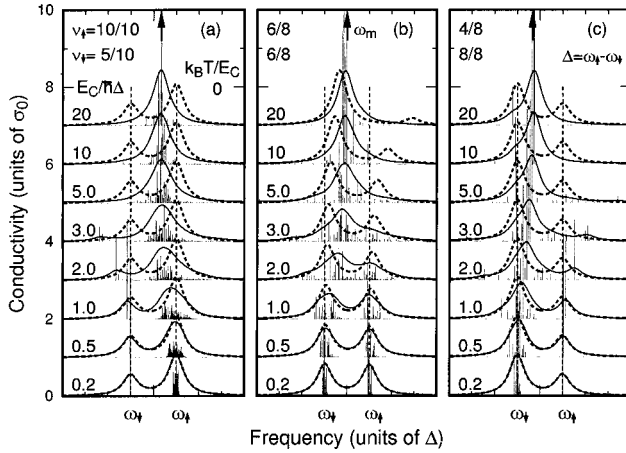


FIG. 8. The α dependence of spin-split CR spectra at $T=0$ for $\nu = \frac{3}{2}$ in four or five hole systems. (a) $(\nu_{\uparrow}, \nu_{\downarrow}) = (1, \frac{1}{2})$, (b) $(\frac{3}{4}, \frac{3}{4})$, and (c) $(\frac{1}{2}, 1)$.

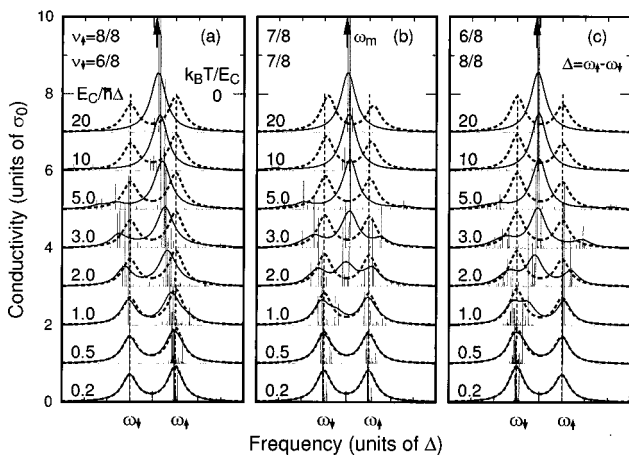


FIG. 9. The α dependence of spin-split CR spectra at $T=0$ for $\nu = \frac{7}{4}$ in two hole systems. (a) $(\nu_{\uparrow}, \nu_{\downarrow}) = (1, \frac{3}{4})$, (b) $(\frac{7}{8}, \frac{7}{8})$, and (c) $(\frac{3}{4}, 1)$.

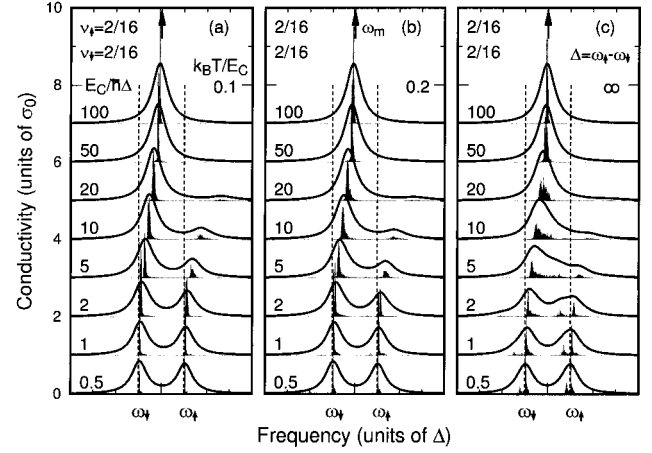


FIG. 10. The α dependence of spin-split CR spectra at $\nu_{\uparrow} = \nu_{\downarrow} = \frac{1}{8}$ for finite temperatures. (a) $k_B T / E_C = 0.1$, (b) 0.2, and (c) ∞ .

ever, they usually have two-peak structures when a sufficiently large broadening is introduced.

Figure 10 shows the dependence of CR spectra on the coupling constant $\alpha = E_C / \hbar \Delta$ for $\nu_{\uparrow} = \nu_{\downarrow} = \frac{1}{8}$ ($\nu = \frac{1}{4}$) at three different temperatures, $k_B T / E_C = 0.1, 0.2$, and ∞ . In this low filling-factor region, qualitative behaviors of CR spectra are insensitive to temperatures and show essentially a positive mode repulsion even at high temperatures, although a signature of a motional narrowing behavior appears in their subpeak structures and in the enhancement of broadening.

Figure 11 shows corresponding results for $(\nu_{\uparrow}, \nu_{\downarrow}) = (\frac{1}{2}, \frac{1}{2})$ ($\nu = 1$). With the increase of the temperature, the spectra change their behavior from a positive mode repulsion to a motional narrowing continuously. Figure 12 shows results for $(\nu_{\uparrow}, \nu_{\downarrow}) = (\frac{3}{4}, \frac{1}{4})$ ($\nu = 1$). In this case, the spectra change their features from a positive mode repulsion to a negative mode repulsion. A crossover occurs at around $k_B T / E_C \sim 0.2$, where they show a motional narrowing. Figure 13 shows results for $(\nu_{\uparrow}, \nu_{\downarrow}) = (\frac{1}{4}, \frac{3}{4})$ ($\nu = 1$), which exhibit a mode-repulsion behavior independent of temperatures although the shifts are suppressed at high temperatures.

This complicated temperature dependence can be understood qualitatively from Fig. 4. With increasing temperature,

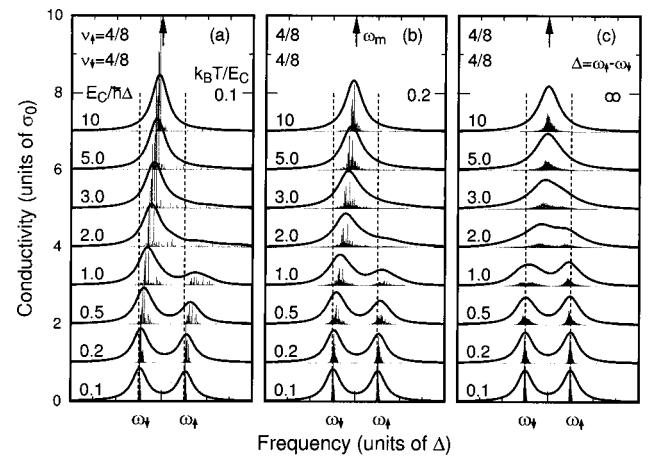


FIG. 11. The α dependence of spin-split CR spectra at $\nu_{\uparrow} = \nu_{\downarrow} = \frac{1}{2}$ for finite temperatures. (a) $k_B T / E_C = 0.1$, (b) 0.2, and (c) ∞ .

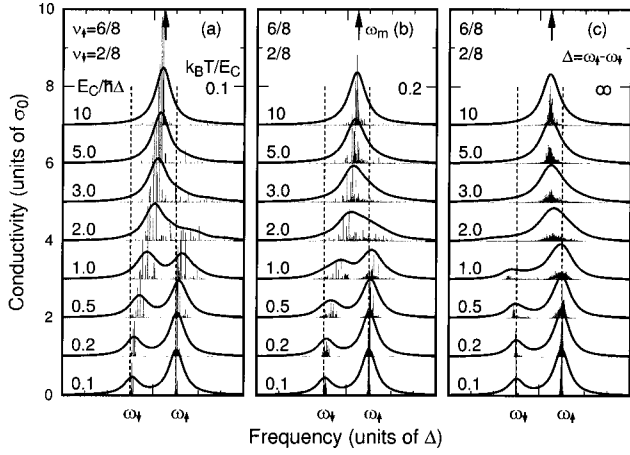


FIG. 12. The α dependence of spin-split CR spectra at $\nu_{\uparrow} = \frac{3}{4}$ and $\nu_{\downarrow} = \frac{1}{4}$ for finite temperatures. (a) $k_B T/E_C = 0.1$, (b) 0.2, and (c) ∞ .

overlapping of wave functions of up- and down-spin electrons becomes appreciable. This means that the temperature increase corresponds roughly to increase in the effective electron concentration at zero temperature, i.e., increase of ν with a fixed $\nu_{\uparrow}/\nu_{\downarrow}$. In fact, for $\nu_{\uparrow} = \nu_{\downarrow} = \frac{1}{2}$, for example, Fig. 4 predicts that the spectra change their behavior from a positive mode repulsion to motional narrowing with increasing ν under the condition $\nu_{\uparrow} = \nu_{\downarrow}$. This qualitatively agrees with the change in the behavior due to the temperature shown in Fig. 11. The same is applicable to the change from a positive to negative mode repulsion in the case $(\nu_{\uparrow}, \nu_{\downarrow}) = (\frac{3}{4}, \frac{1}{4})$ shown in Fig. 12 and to no change in the case $(\frac{1}{4}, \frac{3}{4})$ shown in Fig. 13.

Figure 14 shows the CR spectra in the high-temperature limit ($T \rightarrow \infty$) for the case of a high-filling factor $\nu = \frac{3}{2}$ [$(\nu_{\uparrow}, \nu_{\downarrow}) = (1, \frac{1}{2})$ in (a), $(\frac{3}{4}, \frac{3}{4})$ in (b), and $(\frac{1}{2}, 1)$ in (c)]. The corresponding results at zero temperature are given in Fig. 8. In this case, the characteristic behavior of CR remains essentially independent of temperature, which again agrees quite well with the ν dependence of the zero-temperature CR spectra given in Fig. 4.

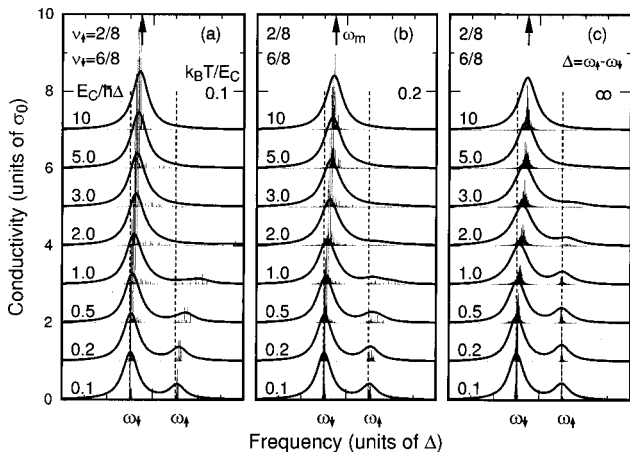


FIG. 13. The α dependence of spin-split CR spectra at $\nu_{\uparrow} = \frac{1}{4}$ and $\nu_{\downarrow} = \frac{3}{4}$ for finite temperatures. (a) $k_B T/E_C = 0.1$, (b) 0.2, and (c) ∞ .

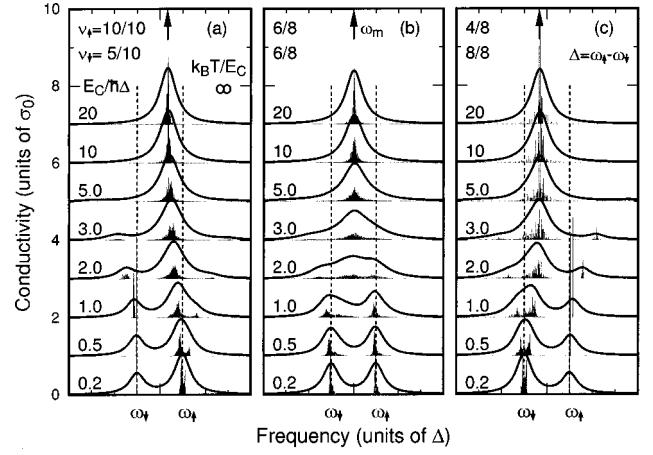


FIG. 14. The α dependence of spin-split CR spectra at $\nu = \frac{3}{2}$ in the high-temperature limit $T \rightarrow \infty$. (a) $(\nu_{\uparrow}, \nu_{\downarrow}) = (1, \frac{1}{2})$, (b) $(\frac{3}{4}, \frac{3}{4})$, and (c) $(\frac{1}{2}, 1)$.

C. Mass-split cyclotron resonance

The calculations are performed under the condition $2 \leq N_0 \leq 7$ and $a/b = 1$ with $N_0 = \text{Min}(N_p, N_h)$. The obtained CR spectra are weakly dependent on N_0 and a/b if $N_0 \geq 4$ and $a/b \sim 1$. The calculated results are shown by the histograms and those obtained by a convolution with a Lorentzian with half-width $\Delta/5$. At absolute zero temperature, the results of GSMA calculation broadened by Lorentzian with width $\Delta/5$ are also shown. The parameters are listed in Table II.

Figure 15 shows the α dependence of the spectra at zero temperature for $\nu_p = \frac{1}{5}, \frac{1}{3},$ and $\frac{3}{4}$. When a sufficiently large broadening is introduced, the spectra exhibit two peak structures and their behavior can be regarded as a ‘‘positive’’ mode repulsion. However, they consist of many δ functions in the region $1 \leq \alpha \leq 10$, showing some deviation from the GSMA results. This deviation from the GSMA result becomes quite appreciable for small values of ν_p but does not for large ν_p .

Figure 16 shows the α dependence of the spectra in the high-temperature limit $T \rightarrow \infty$. The spectra consists of a large number of δ functions but have two-peak structures when a sufficiently large broadening is introduced. Contrary to the case of spin-split CR, the broadened spectra always show a positive mode-repulsion behavior and the effective splitting even seems to increase slightly with temperature.

V. DISCUSSIONS

A. Spin-split cyclotron resonance

The spin-split CR spectra show very rich behaviors depending on filling factors and temperatures. In the limit of

TABLE II. The values of parameters used in the calculations of mass-split CR for the results explicitly shown in the figures.

ν_p	p	N_p	N_h	N_0	N_ϕ
$\frac{1}{5}$	$\frac{1}{3}$	3	12	3	15
$\frac{1}{3}$	0	5	10	5	15
$\frac{3}{4}$	$-\frac{5}{7}$	12	4	4	16

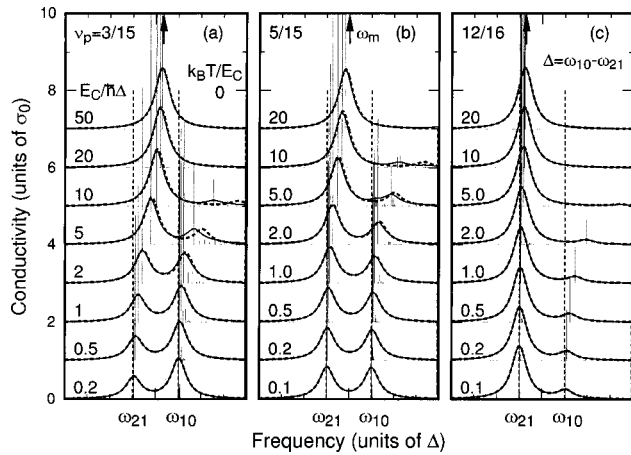


FIG. 15. The α dependence of mass-split CR spectra at $T=0$. (a) $\nu_p = \frac{1}{5}$, (b) $\frac{1}{3}$, and (c) $\frac{3}{4}$.

low filling factors $\nu \ll 1/10$ and low temperatures, guiding centers of electrons are mutually separated and transitions from $N=0$ to $N=1$ can be well approximated as excitations localized around the minimum points of an effective potential formed by electrons with the other spin. This tends to enhance effective cyclotron frequencies of two CR modes and can be regarded as the origin of the positive mode repulsion.

There are many inter-Landau-level excitations other than two optically active collective modes given by Eq. (3.1). However, their coupling with two active modes can be neglected at low filling factors, which is the reason that CR can be reproduced quite well in GSMA. This fact is demonstrated in Appendix B with the use of the theory of Cooper and Chalker.²²

When the filling factor ν is increased, the overlapping between the wave functions of up- and down-spin electrons becomes appreciable and various excitations other than those described by Eq. (3.1) start to contribute to the spectra. For $\nu \lesssim 1$, where a Coulomb hole of size $\sim l$ can still be formed, these excitations give rise to broadening of the peak only and the spectra still show a positive mode repulsion. At higher filling factors $\nu \gtrsim 1$, however, this overlapping starts to change even the basic behavior of the spectra.

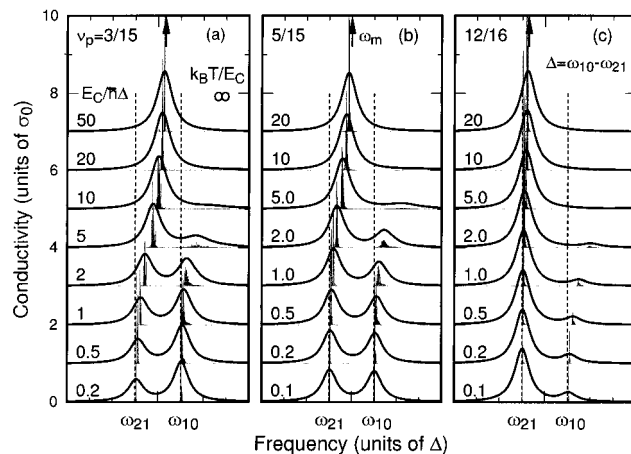


FIG. 16. The α dependence of mass-split CR spectra at $T=\infty$. (a) $\nu_p = \frac{1}{5}$, (b) $\frac{1}{3}$, and (c) $\frac{3}{4}$.

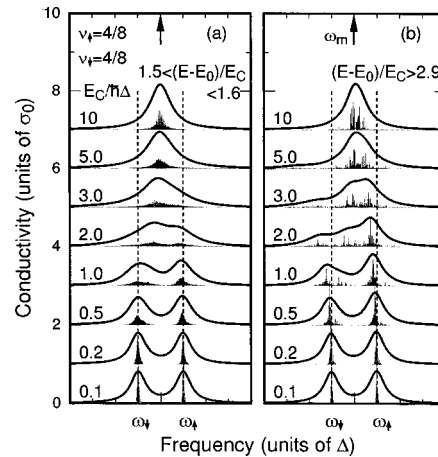


FIG. 17. The spin-split CR for excited states. (a) States with energy $1.5 \leq (E-E_0)/E_C \leq 1.6$; (b) states with energy $(E-E_0)/E_C > 2.9$.

Effects of the overlapping of the wave functions can be demonstrated clearly if we pick up contributions of certain excited states to the dynamical conductivity at low filling factors. We consider the case that $\nu_\uparrow = \nu_\downarrow = \frac{1}{2}$ ($N_e = N_\phi = 8$) for which the spectra exhibit a positive mode-repulsion behavior in the ground state. Figure 17(b) gives the results for the highest ~ 300 excited states [$(E-E_0)/E_C \geq 2.9$, where E is the energy and E_0 is the ground-state energy]. These spectra show a behavior regarded as a negative mode repulsion. This can be understood because CR excitations tend to be localized around “maximum” points of an effective potential created by electrons with other spin and their frequencies tend to be lowered. Figure 17(a) gives the results for ~ 300 excited states lying in the middle of the whole spectra [$1.5 \leq (E-E_0)/E_C \leq 1.6$]. They exhibit a motional narrowing behavior that is considered as a certain average of the positive and negative mode-repulsion because a large number of excitations are coupled with each other in a complicated way with various coupling constants both positive and negative.

The behavior in the region $\nu_\uparrow \sim 1$ and $\nu > 1$ or $\nu_\uparrow \sim 1$ and $\nu > 1$ is exceptional and can be regarded as a mode repulsion. This is presumably because the way of coupling among CR modes is strongly restricted in such cases. Let us consider a situation in which the lowest up-spin Landau level is almost completely filled ($\nu_\uparrow \sim 1$), for example. Figure 18 illustrates processes in which a cyclotron transition is coupled with inter-Landau-level excitations through electron-electron interactions.

The process (a) in which an optically excited up-spin electron decays into down-spin inter-Landau-level excitations is severely limited because of the small number of empty states in the lowest up-spin level. Note that inter-Landau-level transitions between states with a common guiding center, i.e., $\mathbf{q}=0$, are prohibited in the case of electron-electron interactions. On the other hand, the process (b) for optically excited down-spin electrons becomes more and more important with the increase of ν_\uparrow . Consequently, in the case $\nu_\uparrow \ll 1$, CR peaks corresponding to down-spin electrons are repelled to the low-frequency side and their intensity is transferred to that of transitions corresponding to up-spin electrons, leading to a negative mode-repulsion behavior.

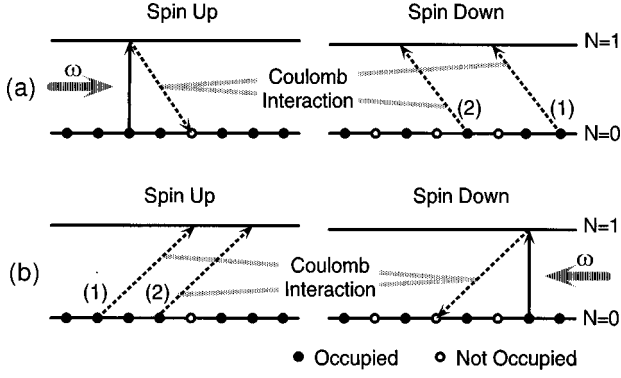


FIG. 18. A schematic illustration of processes in which a cyclotron transition decays into inter-Landau-level excitations for spin-split CR in the case $\nu_{\uparrow} \sim 1$ and $\nu_{\downarrow} < 1$. (a) The up-spin electron excited optically into the $N=1$ Landau level recombines with a hole in the $N=0$ Landau level by exciting a down-spin electron into $N=1$ Landau level through electron-electron interactions. This process is limited by the number of holes in the $N=0$ up-spin Landau level and becomes negligible in the limit $\nu_{\uparrow} \rightarrow 1$. (b) The down-spin electron excited optically recombines with a hole by exciting an up-spin electron into $N=1$ Landau level through interactions. This process remains significant even for $\nu_{\uparrow} \rightarrow 1$.

Note that the process (b) involves states in which same guiding-center coordinates are occupied by electrons in both $N=0$ and 1 Landau levels. These states are completely neglected in GSMA because GSMA considers states in which an electron is excited from the $N=0$ level to $N=1$ with a

common guiding center. This is the main reason that GSMA breaks down in this case. The tendency that GSMA becomes worse for $\nu_{\uparrow} \sim 1$ can be seen also when $\nu=1$ in Fig. 6(a). In principle, GSMA is not valid for $\nu_{\downarrow} \sim 1$ and $\nu=1$, but the deviation is not so apparent because the intensity of the high-frequency peak is too small as shown in Fig. 6(c).

B. Mass-split cyclotron resonance

In the case of mass-split CR, the spectra show only a positive mode-repulsion behavior independent of temperatures and filling factors. The transitions from $N=0$ to $N=1$ occur at the position of a guiding center not occupied by electrons in the $N=1$ Landau level, while the transitions from $N=1$ to $N=2$ occur at a guiding center occupied by electrons. This situation corresponds to spin-split CR for $\nu=1$ at $T=0$, which shows only a positive mode repulsion. In fact, in the ground state at $\nu=1$, up- and down-spin electrons occupy states with different guiding centers because the wave function is given by a single Slater determinant (see Appendix A), and CR transitions for up-spin (down-spin) electrons occur at a guiding center not occupied by down-spin (up-spin) electrons. The relatively large deviation from GSMA at $\nu_p \ll 1$ ($\nu_h \sim 1$) has the same reason for that in spin-split CR at $\nu=1$ and $\nu_{\uparrow} \sim 1$ as discussed above.

C. Relation to experiments

Using parameters of bulk GaAs, characteristic scale values are roughly estimated as follows:¹⁰

$$\text{Cyclotron energy: } \hbar \omega_0 \text{ [meV]} \sim 1.7 \times 10^1 \times (B[\text{T}]/10).$$

$$\text{Coulomb energy: } E_C \text{ [meV]} \sim 1.4 \times 10^1 \times \sqrt{B[\text{T}]/10}.$$

$$\text{Zeeman splitting: } g \mu_B B \text{ [meV]} \sim 2.5 \times 10^{-1} \times (B[\text{T}]/10).$$

$$\text{The difference of cyclotron energy: } \hbar \Delta \text{ [meV]} \sim 5.8 \times 10^{-2} \times (B[\text{T}]/10)^2.$$

$$\text{Temperature: } k_B T \text{ [meV]} \sim 8.6 \times 10^{-2} \times (T[\text{K}]).$$

Under the conditions of usual experiments in magnetic fields $B \sim 10$ T,¹⁷⁻²⁰ the coupling parameter $\alpha = E_C / \hbar \Delta$ has a very large value of the order of 10^2 in GaAs/Al_xGa_{1-x}As heterostructures.

This means that under the usual conditions only a single peak can be observed at $\tilde{\omega} \sim \tilde{\omega}_m = p/2$ in GaAs/Al_xGa_{1-x}As systems even if both up- and down-spin levels are occupied because of strong electron-electron interactions. However, temperature dependence of the CR position gives some information on the spin polarization of the ground state.³¹ In fact, the first moment is expected to decrease from ω_{\uparrow} to $(\omega_{\uparrow} + \omega_{\downarrow})/2$ with the increase of the temperature at $\nu = 1, \frac{1}{3}, \frac{1}{5}, \dots$, where the ground state is a fully spin-polarized state and the spin polarization decreases with the temperature. On the other hand, at $\nu = \frac{2}{3}$, the ground state is spin

unpolarized for $g \leq 0.4$ and the first moment stays at $\omega \sim (\omega_{\uparrow} + \omega_{\downarrow})/2$ at low temperatures.

At low filling factors, CR spectra are well described by those obtained in GSMA. Using the numerical results shown in Fig. 2, the effective coupling parameter is roughly estimated as $\alpha_{\text{eff}} \sim 1$ around at $\nu \sim 1/10$. Thus, the filling factors $\nu = \frac{1}{12}, \frac{1}{9}$, and $\frac{1}{6}$ correspond to weak ($\alpha_{\text{eff}} < 1$), intermediate ($\alpha_{\text{eff}} \sim 1$), and strong ($\alpha_{\text{eff}} > 1$) coupling regimes, respectively. This is the main reason that CR spectra exhibit interesting behaviors only in such a narrow range of ν in GaAs/Al_xGa_{1-x}As heterostructures.

At such low electron concentrations, the spin polarization p is roughly estimated as $p \sim \tanh(g \mu_B B / k_B T)$. Further, the effective coupling constant α_{eff} is expected to depend only weakly on p . Under such assumptions, we can calculate CR

spectra as a function of temperature. This gives exactly the same result reported previously²² and can qualitatively explain experiments. In fact, CR spectra in the weak-coupling regime ($\alpha_{\text{eff}} < 1$) consist of two peaks whose position is weakly dependent on electron-electron interactions, while only a single peak is obtained at $\tilde{\omega} \sim \tilde{\omega}_m$ in the strong coupling regime ($\alpha_{\text{eff}} > 1$). At low temperatures where $p \rightarrow 0$, we have $\tilde{\omega}_+ - \tilde{\omega}_- \rightarrow |1 - \alpha_{\text{eff}}|$ as shown in Eq. (3.7), which means that two peaks come closer together with the decrease of the temperature for $\alpha_{\text{eff}} \sim 1$.

In order to observe characteristic dependence of the cyclotron resonance on the filling factor in the quantum Hall regime predicted in the present work, it is desirable to be able to control effective interaction strength. A bilayer two-dimensional system may be ideal for such purposes.^{32,34-37} In this system, the effective interaction strength can be changed freely by the distance between the layer, the difference of the CR frequency due to nonparabolicity can be modified by the layer thickness, and the relative electron concentration can be controlled by an applied voltage for a gated structure.

VI. SUMMARY AND CONCLUSION

We have numerically studied effects of electron-electron interactions on spin-split and mass-split cyclotron resonance. In the case of spin-split cyclotron resonance, the spectra show very rich behaviors depending on the filling factor of up- and down-spin electrons and on the temperature, i.e., a positive and negative mode-repulsion and motional narrowing behaviors. The results are understood in terms of the characteristic change in the overlapping of wave functions of electrons and the restriction of the available phase space as a function of the filling factor. In the case of mass-split cyclotron resonance, the spectra show only a positive mode-repulsion behavior independent of temperatures and filling factors.

ACKNOWLEDGMENTS

We would like to thank K. Hirakawa, M. Ueda, H. Sakakibara, H. Kino, T. Nakanishi, H. Ajiki, S. Uryu, T. Seri, and H. Matsumura for helpful discussions. This work was supported in part by a Grant-in-Aid for Scientific Research on Priority Area, ‘‘Mesoscopic Electronics: Physics and Technology’’ from the Ministry of Education, Science and Culture, and the Japan Society for the Promotion of Science (‘‘Research for the Future’’ Program JSPS-RFTF96P00103). One of the authors (K.A.) has been supported by the Japan Society for the Promotion of Science for Young Scientists. Some of the numerical calculations were performed on FACOM VPP500 in the Supercomputer Center, Institute for Solid State Physics, University of Tokyo.

APPENDIX A: α_{eff} FOR FULLY SPIN-POLARIZED GROUND STATES

At $\nu = 1, \frac{1}{3}, \frac{1}{5}, \dots$, it is believed that the ground state for a given p is a fully spin-polarized state, i.e.,

$$(\mathbf{S}^{\text{tot}})^2 |\phi_0(p)\rangle = \frac{N_e}{2} \left(\frac{N_e}{2} + 1 \right) \hbar^2 |\phi_0(p)\rangle, \quad (\text{A1})$$

$$S_z^{\text{tot}} |\phi_0(p)\rangle = \frac{pN_e}{2} \hbar |\phi_0(p)\rangle,$$

where \mathbf{S}^{tot} is the total spin operator and S_z^{tot} is its z component. The ground state for $p = 1, |\phi_0(1)\rangle$, can be expanded in the form

$$|\phi_0(1)\rangle = \sum_{X_1 < X_2 < \dots < X_{N_e}} F_{X_1 X_2 \dots X_{N_e}} \times c_{0, X_1, \uparrow}^\dagger c_{0, X_2, \uparrow}^\dagger \dots c_{0, X_{N_e}, \uparrow}^\dagger |\text{vac}\rangle. \quad (\text{A2})$$

Multiplying N_\downarrow times the ladder operator $S_-^{\text{tot}} = S_x^{\text{tot}} - iS_y^{\text{tot}}$, we obtain the ground state for a given p as

$$|\phi_0(p)\rangle = \frac{1}{\sqrt{N_e C_{N_\uparrow}}} \sum_{X_1 < X_2 < \dots < X_{N_e}} \sum_{\sigma_1 \sigma_2 \dots \sigma_{N_e}} \delta_{MN_\downarrow} \times F_{X_1 X_2 \dots X_{N_e}} c_{0, X_1, \sigma_1}^\dagger c_{0, X_2, \sigma_2}^\dagger \dots c_{0, X_{N_e}, \sigma_{N_e}}^\dagger |\text{vac}\rangle, \quad (\text{A3})$$

where $M = \sum_i \delta_{\sigma_i \downarrow}$. Using the formula

$$\left(\sum_{\sigma_1 \dots \sigma_{N_e}} \delta_{MN_\downarrow} \langle \text{vac} | \prod_i c_{0, X_i, \sigma_i} \right) c_{0, X_1, \downarrow}^\dagger c_{0, X_2, \uparrow}^\dagger c_{0, X_3, \uparrow}^\dagger c_{0, X_4, \downarrow}^\dagger \dots c_{0, X_{N_e}, \downarrow}^\dagger \times \left(\sum_{\bar{\sigma}_1 \dots \bar{\sigma}_{N_e}} \delta_{\bar{M}N_\downarrow} \prod_i c_{0, \bar{X}_i, \bar{\sigma}_i}^\dagger |\text{vac}\rangle \right) = N_e - 2 C_{N_\uparrow - 1} \left(\langle \text{vac} | \prod_i c_{0, X_i, \uparrow} \right) \times c_{0, X_1, \uparrow}^\dagger c_{0, X_2, \uparrow}^\dagger c_{0, X_3, \uparrow}^\dagger c_{0, X_4, \uparrow}^\dagger \dots c_{0, X_{N_e}, \uparrow}^\dagger \left(\prod_i c_{0, \bar{X}_i, \uparrow}^\dagger |\text{vac}\rangle \right), \quad (\text{A4})$$

$$(X_1 < X_2 < \dots < X_{N_e} \text{ and } \bar{X}_1 < \bar{X}_2 < \dots < \bar{X}_{N_e}),$$

the projected structure factor between up- and down-spin electron is calculated as

$$S_{\uparrow\downarrow}(\mathbf{q}) = \frac{1}{N_\phi} \langle \phi_0(p) | \rho_\uparrow^{00}(\mathbf{q}) \rho_\downarrow^{00}(-\mathbf{q}) | \phi_0(p) \rangle = \frac{N_e - 2 C_{N_\uparrow - 1}}{N_e C_{N_\uparrow}} S_0(\mathbf{q}) = \frac{N_\uparrow N_\downarrow}{N_e (N_e - 1)} S_0(\mathbf{q}), \quad (\text{A5})$$

where $S_0(\mathbf{q})$ is defined by

$$S_0(\mathbf{q}) = \frac{1}{N_\phi} [\langle \phi_0(1) | \rho_\uparrow^{00}(\mathbf{q}) \rho_\uparrow^{00}(-\mathbf{q}) | \phi_0(1) \rangle - N_e]. \quad (\text{A6})$$

Thus, α_{eff} is independent of p and written as

$$\alpha_{\text{eff}} = -\frac{1}{N_\phi} \sum_{\mathbf{q}} \frac{N_\phi}{N_e - 1} S_0(\mathbf{q}) \frac{|\mathbf{q}|l}{2} \exp\left(-\frac{|\mathbf{q}|^2 l^2}{2}\right). \quad (\text{A7})$$

At $\nu=1$ ($m=0$), in particular, $S_0(\mathbf{q})$ can be calculated analytically³⁸ as

$$S_0(\mathbf{q}) = N_e \delta'_{\mathbf{q}} - 1, \quad (\text{A8})$$

and we get $\alpha_{\text{eff}} = \sqrt{\pi/8}$ in the limit $N_e \rightarrow \infty$ and $N_\phi \rightarrow \infty$.

APPENDIX B: RELATIONSHIP BETWEEN COOPER AND CHALKERS' THEORY AND GSMA

In the extreme quantum limit characterized by $\nu \ll 1/10$, the ground state is a Wigner solid state $|\phi_0\rangle$. Because exchange interaction is very small, electrons can be regarded as distinguishable particles. The inter-Landau-level transition operator for i th electron is defined by

$$a_i^\dagger = \frac{1}{\sqrt{2}l} (u_i^x + iu_i^y), \quad (\text{B1})$$

using the relative coordinate $\mathbf{u}_i = \mathbf{r}_i - \mathbf{R}_i$. In Ref. 22, the equation of motion for a_i^\dagger is expanded with respect to l/d , where d is the lattice constant of the Wigner solid. This leads to

$$[\mathcal{H}, a_i^\dagger] = \hbar \omega_{\sigma_i} a_i^\dagger + \frac{E_C}{2} \left(\frac{l}{d}\right)^3 \sum_j M_{ij} a_j^\dagger, \quad (\text{B2})$$

where M_{ij} is defined by

$$M_{ij} = \begin{cases} \sum_{k \neq i} \left(\frac{d}{|\mathbf{R}_i - \mathbf{R}_k|}\right)^3 & (i=j), \\ -\left(\frac{d}{|\mathbf{R}_i - \mathbf{R}_j|}\right)^3 & (i \neq j). \end{cases} \quad (\text{B3})$$

Noting that

$$A_{0\sigma}^+ |\phi_0\rangle = \sum_{i(\sigma_i=\sigma)} a_i^\dagger |\phi_0\rangle, \quad (\text{B4})$$

we obtain

$$\begin{aligned} [\mathcal{H}, A_{0\sigma}^+] |\phi_0\rangle &= \hbar \omega_{\sigma} A_{0\sigma}^+ |\phi_0\rangle \\ &+ \frac{E_C}{2} \left(\frac{l}{d}\right)^3 \left[- \sum_{i(\sigma_i=\sigma)} \sum_{j(\sigma_j \neq \sigma)} M_{ij} a_i^\dagger \right. \\ &\left. + \sum_{i(\sigma_i \neq \sigma)} \sum_{j(\sigma_j \neq \sigma)} M_{ij} a_j^\dagger \right] |\phi_0\rangle. \end{aligned} \quad (\text{B5})$$

Because up-spin and down-spin electrons are randomly placed,

$$\begin{aligned} \sum_{i(\sigma_i=\sigma)} \sum_{j(\sigma_j \neq \sigma)} M_{ij} a_i^\dagger |\phi_0\rangle &\sim \frac{1}{N_\sigma} \sum_{i(\sigma_i=\sigma)} \sum_{j(\sigma_j \neq \sigma)} M_{ij} A_{0\sigma}^+ |\phi_0\rangle \\ &\sim \frac{\nu_\uparrow \nu_\downarrow}{\nu_e \nu_\sigma} \lambda A_{0\sigma}^+ |\phi_0\rangle, \end{aligned}$$

$$\begin{aligned} \sum_{i(\sigma_i \neq \sigma)} \sum_{j(\sigma_j \neq \sigma)} M_{ij} a_j^\dagger |\phi_0\rangle &\sim \frac{1}{N_{\bar{\sigma}}} \sum_{i(\sigma_i \neq \sigma)} \sum_{j(\sigma_j \neq \sigma)} M_{ij} A_{0\bar{\sigma}}^+ |\phi_0\rangle \\ &\sim \frac{\nu_\uparrow \nu_\downarrow}{\nu_e \nu_{\bar{\sigma}}} \lambda A_{0\bar{\sigma}}^+ |\phi_0\rangle, \end{aligned} \quad (\text{B6})$$

where $\bar{\sigma}$ is the reversed spin state of σ and λ is a constant defined by

$$\lambda = \sum_{\mathbf{l} \neq 0} |\mathbf{l}|^{-3}, \quad (\text{B7})$$

with $\mathbf{l} = (n + m/2, \sqrt{3}m/2)$ (n, m : integer). Consequently, two CR modes defined by Eq. (3.1) are coupled only with each other and decoupled with other inter-Landau-level excitations. The spectra are well reproduced by GSMA and calculated from the effective Hamiltonian (3.2). The effective coupling constant can be calculated as Eq. (3.14).

-
- ¹W. Kohn, Phys. Rev. **123**, 1242 (1961).
²H. Küblbeck and J. P. Kotthaus, Phys. Rev. Lett. **35**, 1019 (1975).
³P. Stallhofer, J. P. Kotthaus, and J. F. Koch, Solid State Commun. **20**, 519 (1976).
⁴G. Abstreiter, P. Stallhofer, and J. P. Kotthaus, Surf. Sci. **98**, 413 (1980).
⁵P. Stallhofer, J. P. Kotthaus, and G. Abstreiter, Solid State Commun. **32**, 655 (1979).
⁶T. Ando, in *Lecture Notes of the International Conference on the Application of High Magnetic Fields in Semiconductor Physics, Würzburg, 1976*, edited by G. Landwehr (Universität Würzburg, Würzburg, 1976), p. 33.
⁷Y. Takada and T. Ando, J. Phys. Soc. Jpn. **44**, 905 (1978).
⁸Y. Takada, Surf. Sci. **98**, 442 (1980).
⁹J. Appel and A. W. Overhauser, Phys. Rev. B **18**, 758 (1978).
¹⁰See, for example, M. A. Hopkins, R. J. Nicholas, P. Pfeffer, W. Zawadzki, D. Gauthier, J. C. Portal, and M. A. DiForte-Piosson, Semicond. Sci. Technol. **2**, 568 (1987).
¹¹See, for example, G. Lindemann, R. Lassnig, W. Seidenbusch, and E. Gornik, Phys. Rev. B **28**, 4693 (1983).
¹²F. Thiele, U. Merkt, J. P. Kotthaus, G. Lommer, F. Malcher, U. Rössler, and G. Weimann, Solid State Commun. **62**, 841 (1987) and references therein.
¹³K. Ensslin, D. Heitmann, H. Sigg, and K. Ploog, Phys. Rev. B **36**, 8177 (1987) and references therein.
¹⁴E. Batke, H. L. Störmer, A. C. Gossard, and J. H. English, Phys. Rev. B **37**, 3093 (1988) and references therein.
¹⁵C. M. Hu, E. Batke, K. Köhler, and P. Ganser, Phys. Rev. Lett. **75**, 918 (1995).
¹⁶C. M. Hu, E. Batke, K. Köhler, and P. Ganser, Phys. Rev. Lett. **76**, 1904 (1996).
¹⁷M. Besson, E. Gornik, C. M. Engelhardt, and G. Weimann, Semicond. Sci. Technol. **7**, 1274 (1992).
¹⁸C. M. Engelhardt, E. Gornik, M. Besson, G. Böhm, and G. Weimann, Surf. Sci. **305**, 23 (1994).
¹⁹G. M. Summers, R. J. Warburton, J. G. Michels, R. J. Nicholas, J. J. Harris, and C. T. Foxon, Phys. Rev. Lett. **70**, 2150 (1993).
²⁰J. G. Michels, S. Hill, R. J. Warburton, G. M. Summers, P. Gee,

- J. Singleton, R. J. Nicholas, C. T. Foxon, and J. J. Harris, *Surf. Sci.* **305**, 33 (1994).
- ²¹R. J. Nicholas, D. J. Barnes, N. Miura, C. T. Foxon, and J. J. Harris, *J. Phys. Soc. Jpn.* **62**, 1267 (1993).
- ²²N. R. Cooper and J. T. Chalker, *Phys. Rev. Lett.* **72**, 2057 (1994).
- ²³P. Johansson, *Phys. Rev. B* **50**, 14 734 (1994).
- ²⁴A. H. MacDonald and C. Kallin, *Phys. Rev. B* **40**, 5795 (1989).
- ²⁵K. Asano and T. Ando, *J. Phys. Soc. Jpn.* **65**, 1191 (1996).
- ²⁶D. Yoshioka, *Phys. Rev. B* **29**, 6833 (1984).
- ²⁷D. Yoshioka, *J. Phys. Soc. Jpn.* **55**, 885 (1986).
- ²⁸D. Yoshioka, *J. Phys. Soc. Jpn.* **55**, 3960 (1986).
- ²⁹F. D. M. Haldane, *Phys. Rev. Lett.* **55**, 2095 (1985).
- ³⁰M. Kasner and A. H. MacDonald, *Phys. Rev. Lett.* **76**, 3204 (1996).
- ³¹T. Chakraborty and P. Pietiläinen, *Phys. Rev. Lett.* **76**, 4018 (1996).
- ³²A. H. MacDonald and S.-C. Zhang, *Phys. Rev. B* **49**, 17 208 (1994).
- ³³L. Bonsall and A. A. Maradudin, *Phys. Rev. B* **15**, 1959 (1977).
- ³⁴K. Ensslin, D. Heitmann, M. Dobers, K. von Klitzing, and K. Ploog, *Phys. Rev. B* **39**, 11 179 (1989).
- ³⁵A. Lorke, U. Merkt, F. Malcher, G. Weimann, and W. Schlapp, *Phys. Rev. B* **42**, 1321 (1990).
- ³⁶Y. B. Vasilyev, D. Bertram, M. Dilger, K. von Klitzing, and K. Eberl, in *High Magnetic Fields in Physics of Semiconductors II*, Proceedings of the 12th International Conference on the Application of High Magnetic Fields in Semiconductor Physics, Würzburg, 1996, edited by G. Landwehr and W. Ossau (World Scientific, Singapore, 1997), Vol. 2, p. 781.
- ³⁷H. Sakakibara and K. Hirakawa, *Physica B* (to be published).
- ³⁸R. B. Laughlin, *Phys. Rev. Lett.* **50**, 1395 (1983).